

Chromatographic Study of Alkanes in Silicalite: Transport Properties

Jeffrey R. Hufton and Ronald P. Danner

Dept. of Chemical Engineering, The Pennsylvania State University, University Park, PA 16802

Micropore diffusion coefficients for infinitely-dilute methane, ethane, propane, n-butane, and isobutane in silicalite were measured via concentration-pulse chromatography. Two different samples of large laboratory-synthesized crystals were investigated. Analysis of van Deemter plots clearly indicated the presence of a significant micropore mass-transfer resistance for isobutane. Diffusion coefficients evaluated from these plots were consistent with results measured by the membrane technique. The linear alkane data differed completely in that the micropore mass-transfer resistance for these adsorbates was very small, implying that the true diffusion coefficients were too large to be measured with this system. Thus, effective diffusion coefficients evaluated from these data represent a lower limit of the true values. Comparison of this limit with nuclear magnetic resonance data was favorable, since the latter are significantly larger in magnitude. Inconsistency was observed with diffusion coefficients obtained from other macroscopic techniques including the membrane method, zero-length and tracer-pulse chromatography, and some frequency response experiments.

Introduction

Knowledge of the transport rate of adsorbate through a solid adsorbent is often crucial for the accurate design of adsorption-based separation units. In an equilibrium separation, transport properties determine the shape of the breakthrough curve or the concentration history at the column outlet. For the case of negligible mass-transfer resistances, the breakthrough curve is represented mathematically by a step function at time t_b . Separation units are efficiently operated with a cycle time slightly less than t_b . If mass-transfer limitations are present, however, the breakthrough curve will become skewed and adsorbed components will exit the column earlier than t_b . Thus, if mass-transfer resistances are significant but ignored during the design of an adsorption unit, then operation at the proposed cycle time will result in reduced product purity. This problem can be alleviated to some extent by decreasing the cycle time, but the overall system design will not be optimal in this case.

Transport phenomena can also be the foundation of adsorption-based separation processes, that is, kinetic separa-

tions. For example, oxygen and nitrogen are obtained from air via a kinetic separation on carbon molecular sieve adsorbent (Knoubach, 1978). The difference between the rates of diffusion through the solid results in separation; the slowly diffusing component remains primarily in the gas, while the quickly diffusing adsorbate is held up in the adsorbent phase. Accurate transport data are required for the complete design of both equilibrium and kinetic separation processes.

Transport mechanisms which result in the spreading of the concentration front include axial dispersion, external mass transfer, and micropore and macropore diffusion. Axial dispersion accounts for flow through the packed bed, and external mass transfer characterizes the transport of adsorbate from the bulk gas to the adsorbent surface. Micropore and macropore diffusion refer to transport through the very narrow channels of the adsorbent crystals and the interstitial passages between these crystals, respectively. The latter arise since zeolite crystals are combined to form pellets for industrial applications; this necessarily results in the formation of a bidisperse pore structure.

The degree of spreading resulting from the above mecha-

Correspondence concerning this article should be addressed to R. P. Danner.

J. R. Hufton is presently at the Department of Chemical Engineering, University of New Brunswick, Fredericton, NB, Canada E3B 5A3.

nisms, excluding micropore diffusion, can be minimized to some extent by adjusting either the gas flow rate or pellet size. Since commercial zeolite crystal sizes are fairly constant, the micropore process is essentially fixed once the adsorbate, adsorbent, and column conditions are set. If micropore effects are significant, then the overall transport resistance will still be substantial even if the other mechanisms are diminished by judicious choice of operating parameters. Hence, it is important to determine this transport resistance during early stages of the design process.

Many different experimental techniques have been devised for determining diffusion coefficients in gas/solid systems. They have been described and discussed by Ruthven (1984), Kärger and Ruthven (1989), and Chang and Dooley (1990). Kärger and Ruthven (1989) classified the various techniques into two groups—macroscopic and microscopic. Classification is determined by how the measurements are carried out. In macroscopic techniques, the diffusion coefficients are determined by measuring the effect of adsorbed-phase diffusion on a macroscopic variable (for example, gas pressure or adsorbent weight). In general, the duration of the measurement is of the order of seconds or more. Conversely, microscopic measurements monitor the travel of adsorbate on a molecular level, and the measurements are typically on the order of a few milliseconds. Additionally, microscopic techniques measure the self-diffusion coefficient, whereas macroscopic techniques usually, but not always, measure transport diffusion coefficients.

The most common macroscopic experiment reported in the literature is the sorption uptake (SU) method. In this technique, the adsorbed-phase weight, gas-phase pressure at constant volume, or gas-phase volume at constant pressure is measured as a function of time after a step change in the gas-phase composition has been made. Comparison of the shape of this response with a suitable mathematical model allows determination of the micropore diffusion coefficient. This technique has been criticized because the rate of heat transfer resulting from the exothermic adsorption process frequently controls the system kinetics (Ruthven, 1984, p. 189; Kärger and Ruthven, 1981, 1989).

The general method of perturbation chromatography is to introduce some type of pulse to a previously equilibrated chromatographic system and measure the response. The evolution of the pulse can be described mathematically, and various mass-transfer parameters contained therein can be determined by comparison with the experiments. Various versions of this method have been used, the most common being concentration pulse chromatography (CPC). In this technique, a pulse of adsorbate is injected into an inert carrier gas which passes through a packed column and, eventually, the detectors. This type of experiment was used in this study; therefore, it will be described in more detail in a later section.

An offshoot of the perturbation chromatography method was developed by Ruthven and coworkers (Eic and Ruthven, 1988, 1989; Eic et al., 1988). Termed zero-length chromatography (ZLC), it was designed to eliminate or drastically reduce auxiliary mass-transfer resistances observed during CPC experiments (axial dispersion, macropore, and external mass-transfer resistances). A few milligrams of adsorbent is placed in a "column" and equilibrated with an inert gas stream containing a small amount of adsorbate. At the beginning of the

experiment, the feed stream is diverted and replaced with pure inert stream at a high flow rate. A detector at the outlet of the column measures the gas-phase concentration as a function of time, and a desorption curve is produced. Comparison with a theoretical model enables the determination of mass-transfer parameters.

Another method is a variation of the common Wicke-Kallenbach experiment, referred to here as the membrane technique (MBR) (Paravar and Hayhurst, 1983; Wernick and Osterhuber, 1983). The essentially steady-state transport of adsorbate is measured in this technique. A single large zeolite crystal is mounted in a rigid support plate, and both sides of the sample are evacuated. An experimental run is initiated by introducing relatively low-pressure adsorbate to one side of the membrane. Diffusion of adsorbate through the crystal increases the gas pressure of the other cavity. Since this pressure never attains a very large value, it can be assumed to be zero with respect to the diffusion equation. The rate of the pressure increase is proportional to the "steady-state" flux of adsorbate from which an estimation of the micropore diffusion coefficient can be obtained.

The frequency response method (FR) is a macroscopic technique initially developed in Japan (Yasuda, 1982; Yasuda and Sugawara, 1984). The experiment is carried out by sinusoidally varying the volume of a chamber containing equilibrated adsorbent and adsorbate. The phase angle and amplitude of the oscillating pressure are recorded as a function of the frequency of the volume perturbations. Micropore diffusion coefficients are obtained by comparing with a mathematical model. This technique is rather unique in that the time interval for measurement can be varied by changing the frequency of the oscillations.

The pulsed field gradient nuclear magnetic resonance (PFG-NMR) experiment developed by Kärger and Pfeifer (1987, 1988) and Kärger et al. (1983) is the most common microscopic technique for measuring micropore diffusion coefficients. This method utilizes NMR principles to monitor the displacement of molecules in an equilibrated system. By measuring the rate of transport in the absence of concentration gradients, the self-diffusion coefficient of the adsorbate is obtained. Experimental difficulties related to the relaxation of the nuclear spins limit application of the technique to relatively fast systems.

The quasi-elastic neutron scattering technique (QENS) is another microscopic experiment which can be used to determine micropore diffusion coefficients (Jobic et al., 1989, 1992). As in the NMR method, only adsorbates with rather high self-diffusion coefficients can be analyzed.

Discrepancies between diffusion coefficients measured by PFG-NMR and other macroscopic techniques have been discussed in the literature ever since the former technique was first applied to zeolitic systems (mid-1970s). The first "reviews" concerning this subject were made by Kärger and Caro (1977) and Ruthven (1977). Both illustrated discrepancies of three or four orders of magnitude in the light alkane/5A and heptane and benzene/13X systems. The reasons for these were thought to be either surface barrier effects (Kärger and Caro) or possible inadequacies of the PFG-NMR technique (Ruthven). Remarkable qualitative consistencies were demonstrated, however, such as the trend of the diffusion coefficients with concentration or cation loading. Kärger and Caro additionally presented results that confirmed the validity of the PFG-NMR

techniques and carried out experiments with water and methane in large natural chabazites which agreed with uptake studies.

Kärger and Ruthven (1981) compared PFG-NMR and gravimetric results for similar batches of larger synthetic 5A and 13X zeolite crystals. Good agreement and self-consistency were obtained for *n*-butane and propane in 5A and triethylamine in 13X. Diffusion coefficients of benzene in 13X as measured by sorption uptake, however, were lower than the PFG-NMR results and exhibited a strange concentration dependence. Slight differences in regeneration technique were thought to be possibly responsible. (Bülow et al., 1983, later showed that the discrepancy was attributable to external time delays in the sorption experiments.) An important result of this work was the realization that zeolite dehydration processes can be very important; the diffusion coefficient of *n*-butane in commercial 5A zeolite was two orders of magnitude lower than in laboratory-synthesized crystals.

The most recent discussion of the discrepancy topic is that of Kärger and Ruthven (1989). These authors methodologically analyzed different experimental techniques and tabulated more reliable results for diffusion in 4A, 5A, 13X, and silicalite/ZSM-5 zeolites. A key finding was that agreement was obtained with the slower systems, and conversely, disagreement occurred for quickly diffusing adsorbates. After extensive consideration of the commonly postulated reasons, they concluded that the difference in time scales of the measurements results in the observed discrepancies. A "dual-mode" description of diffusion, where both mobile and immobile states exist in the solid, was hypothesized. This model, however, was not completely consistent with the PFG-NMR results.

A substantial amount of work has been directed toward the measurement of micropore diffusion coefficients in silicalite. The usefulness of a structurally-identical material, ZSM-5, in catalysis prompted studies of aromatics, ethers, and higher molecular weight alkanes in this material (for example, Doelle et al., 1981; Wu et al., 1983; Ma and Savage, 1987; Zikanova et al., 1987; Shah et al., 1988; Qureshi and Wei, 1990). Emphasis has also been placed on the behavior of lighter alkanes in silicalite. Diffusion coefficients have been measured via concentration pulse (Chiang et al., 1984) and tracer pulse chromatography (TPC; Hufton and Danner, 1991) with small commercial crystals, PFG-NMR (Caro et al., 1985; Kärger et al., 1986), QENS (Jobic et al., 1989, 1992), the frequency response method (Bülow et al., 1986a; Van den Begin et al., 1989; Van den Begin and Rees, 1989), sorption uptake (Bülow et al., 1986a,b), the membrane technique (Paravar and Hayhurst, 1983; Hayhurst and Paravar, 1988), and ZLC (Eic and Ruthven, 1989). Comparison of these data for a given adsorbate (such as propane) shows discrepancies of up to six orders of magnitude! In general, diffusion coefficients obtained from MBR, ZLC, TPC, and some of the FR experiments are in reasonable agreement (Eic and Ruthven, 1989). The CPC data are a few orders of magnitude lower than this, and the PFG-NMR and QENS results roughly two orders higher. Some agreement with the latter values has been obtained in revised FR experiments with much smaller adsorbent samples.

The objective of this work was to determine micropore diffusion coefficients of methane, ethane, propane, *n*-butane and isobutane on two different samples of large laboratory-synthesized silicalite crystals by CPC. Experiments were carried out at infinite dilution, where the self- and transport-diffusion

coefficients become equivalent (neglecting any zeolite relaxation effects). Thus, the calculated diffusion coefficients can be directly compared with self-diffusion coefficients obtained by microscopic techniques—correction via the Darken equation is unnecessary (Ruthven, 1984, p. 127). Additional goals were to determine the effect of alkane length and branching on the rate of diffusion and to begin to investigate consequences of the anisotropic nature of the silicalite channels.

Theory

Many investigators have used CPC to estimate transport properties of adsorbates in solid adsorbents. These include, but are not limited to, Schneider and Smith (1968), Ma and Mancel (1972), Hashimoto and Smith (1973), Shah and Ruthven (1977), Chihara et al. (1978), Ruthven and Kumar (1979), Hsu and Haynes (1981), Chiang et al. (1984a,b), Boniface and Ruthven (1985), and Fu et al. (1986). Further description of some of the key developments in CPC (and TPC) can be found in the thesis of Hufton (1992). Practical aspects of the technique are discussed by Helfferich and Klein (1970), Conder and Young (1979), and Ruthven (1984).

The technique is rather simple in principle—the evolution of a pulse of adsorbate in a packed column is compared with a mathematical model of the system, thereby enabling the determination of transport parameters contained in the model. The simplest example of this technique is CPC at infinite dilution, for it is very similar to the familiar analytical chromatography technique. This also happens to be the mode of experimentation used in this study. In this case, a small pulse of adsorbate is injected into an inert carrier gas (usually helium) which passes through the packed column. Detectors at the column outlet measure the time-dependent concentration, resulting in a chromatographic peak.

Proper analysis of this peak requires a mathematical model of the system which includes all of the important transport processes associated with the experimental system. Two procedures have been frequently used to compare experimental results with theory—the method of moments and time- (or frequency-) domain analysis. Previous authors (Haynes, 1975; Wakao et al., 1980; Radeke, 1981; Fahim and Wakao, 1982; Ruthven, 1984) have generally recommended use of the latter technique, with first estimates provided by the simple moments method. In this study, the moments method was used to obtain parameters which were later validated with time domain comparisons.

Moments method

Transport properties are determined from the second moment or variance of the chromatographic peak. This can be calculated from numerical peak data by integrating the following expression:

$$\sigma^2 = \frac{\int_0^\infty (t - t_R)^2 C(t) dt}{\int_0^\infty C(t) dt} \quad (1)$$

The first moment or retention time of the peak (t_R) is also calculated by integration (Hufton and Danner, 1993). A sim-

pler expression for estimating the second moment is given by Conder and Young (1979, p. 82):

$$\sigma^2 = 0.1803 w_{1/2}^2 \quad (2)$$

The value of $w_{1/2}$ is readily obtained from chromatographic peaks, since it is just the peak width at a peak height equal to half of the maximum. This approximation is strictly valid for Gaussian peaks only, so it is not surprising that Schneider (1987) has shown this relationship to be erroneous for significantly tailed peaks. The detector responses measured during this study, however, were nearly symmetric, so the approximation made in Eq. 2 is justifiable. Random comparisons with moments determined via Eq. 1 were used to confirm this assumption.

The analysis procedure employed in this study is significantly simpler than that in previous studies, since the column was packed directly with adsorbent crystals. Thus, the macropore resistance term can be omitted from the second moment expression. The following expression for the second moment is based on work by Haynes and Sarma (1973) and Shah and Ruthven (1977):

$$\sigma^2 = \frac{2L}{U_o} D_t \left[1 + \frac{(1-\epsilon)}{\epsilon} K \right]^2 + \frac{2L}{U_o} \frac{(1-\epsilon)}{\epsilon} \left[\frac{K^2 R_p}{3k_f} + \frac{K \langle R_c^2 \rangle}{15D} \right] \quad (3)$$

where the macropore term and ϵ_p have been eliminated. The average value of the squared crystal radius, $\langle R_c^2 \rangle$, is calculated from the volume-averaged effective crystal radius distribution, $f(R_c)$:

$$\langle R_c^2 \rangle = \int_0^\infty R_c^2 f(R_c) dR_c \quad (4)$$

Equation 3 includes terms characterizing axial dispersion, external mass transfer, and micropore diffusion resistances. A conservative estimate of k_f can be obtained using a limit of the Sherwood number equal to 2 at low carrier gas velocity (Wakao and Funazkri, 1978; Ruthven, 1984, p. 246). The value of k_f then becomes equal to D_m/R_p , which is substituted into Eq. 3. Comparison of this external mass-transfer term with experimental data, though, indicated that it was negligible (less than 1% of micropore resistance). Thus, it was neglected in the development of the moment equations.

Equation 3 can be rearranged into the following useful form (Ma and Mancel, 1973; Hashimoto and Smith, 1973; Hufton and Danner, 1991):

$$\frac{\sigma^2 U_o}{2L} = \frac{D_t}{U_o^2} \left[1 + \frac{(1-\epsilon)}{\epsilon} K \right]^2 + \frac{(1-\epsilon)}{\epsilon} \frac{K \langle R_c^2 \rangle}{15D} \quad (5)$$

The axial dispersion coefficient is at most proportional to the interstitial gas velocity (Edwards and Richardson, 1968; Suzuki and Smith, 1972), so at high values of U_o the axial dispersion term is negligible. Thus, the micropore diffusion coefficient can be obtained from the intercept of plots of $\sigma^2 U_o / 2L$ vs. $1/U_o^2$ (referred to as variance plots). The axial dispersion coefficient can be estimated from the local slope of these data. Calculation of both quantities requires knowledge of the Hen-

ry's constants, K , which are obtained from analysis of first moments (Hufton and Danner, 1993).

Another common method for analyzing second moment data is the van Deemter approach (Van Deemter et al., 1956). The height equivalent to a theoretical plate (HETP) is defined from Eq. 5 as:

$$\text{HETP} = \frac{\sigma^2}{f_1^2} L = \frac{2D_t}{U_o} + 2 \frac{\epsilon}{(1-\epsilon)} \frac{\langle R_c^2 \rangle}{15KD} U_o \quad (6)$$

At high gas velocities, the righthand side of this equation is dominated by the second term. The value of D is obtained from the slope of a plot of HETP vs. U_o at high gas velocities, m :

$$D = \frac{2}{15} \frac{\epsilon}{(1-\epsilon)} \frac{\langle R_c^2 \rangle}{K m} \quad (7)$$

High carrier gas velocities in a packed column often result in significant column pressure drop. To permit proper analysis of the experimental data, this effect must be accounted for in the theoretical model. When pressure drop is significant, the gas velocity, gas concentration, and axial dispersion coefficient (through the molecular diffusion coefficient) vary with axial position in the column. Chiang et al. (1984a) extended the early nonisobaric works of James and Martin (1952), Giddings (1965), and Carleton et al. (1978); a simplified version of their expression in terms of the HETP is:

$$\frac{\text{HETP}}{f_1} = \frac{2D_t}{U_o} + \frac{2}{15} \frac{\epsilon}{(1-\epsilon)} \frac{\langle R_c^2 \rangle}{KD} \left(\frac{U_o}{f_1 f_2} \right) \quad (8)$$

where

$$f_1 = \frac{9}{8} \frac{\left[\left(\frac{P_i}{P_o} \right)^2 - 1 \right] \left[\left(\frac{P_i}{P_o} \right)^4 - 1 \right]}{\left[\left(\frac{P_i}{P_o} \right)^3 - 1 \right]^2} \quad (9)$$

$$f_2 = \frac{2}{3} \frac{\left(\frac{P_i}{P_o} \right)^3 - 1}{\left(\frac{P_i}{P_o} \right)^2 - 1} \quad (10)$$

Thus, the slope of a plot of HETP/f_1 vs. $U_o/(f_1 f_2)$ at high velocities can be used to determine the micropore resistance from nonisobaric data.

Time-domain analysis

Derivation of the moment expressions requires formulation of the adsorbate concentration at the column exit in the Laplace domain. Transformation of Laplace functions into the time domain is possible via the standard inversion formula:

$$f(t) = \frac{1}{2\pi i} \int_{a-i\infty}^{a+i\infty} e^{st} f(s) ds \quad (11)$$

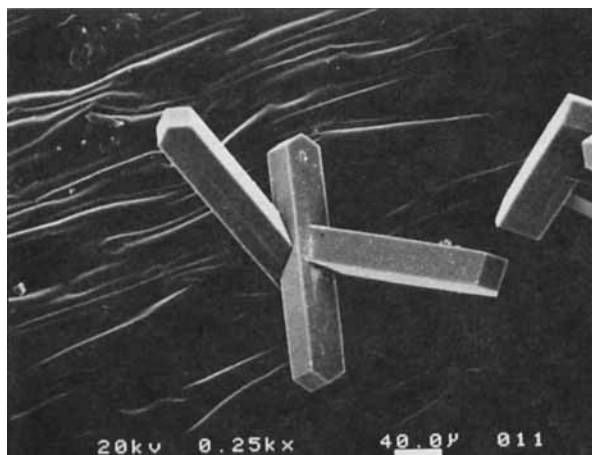


Figure 1. Scanning electron microscopy of silicalite sample A.

where i represents the complex number $\sqrt{-1}$. The complex integration of the Laplace domain concentration expression has been developed and discussed by Rasmuson (1981, 1982, 1985) and Rasmuson and Neretnieks (1980). For an infinitely dilute, isobaric system containing only micropore diffusion and axial dispersion effects and described by a pulse inlet condition (Eq. 5 in moment method), the following expression for $C(t, L)$ results:

$$\frac{C(t, L)}{\int_0^\infty C dt} = \frac{2y}{\pi} \int_0^\infty \exp \left[\frac{Pe}{2} - \sqrt{\frac{A^2 + B^2 + A}{2}} \right] \times \cos \left[y\lambda^2 t - \sqrt{\frac{A^2 + B^2 - A}{2}} \right] \lambda d\lambda \quad (12)$$

where

$$A = Pe \left(\frac{Pe}{4} + \delta H_1(\lambda) \right)$$

$$B = \frac{2}{3} \frac{\delta \lambda^2 Pe}{R_1} + \delta H_2(\lambda) Pe$$

$$H_1(\lambda) = \lambda \left[\frac{\sinh(2\lambda) + \sin(2\lambda)}{\cosh(2\lambda) - \cos(2\lambda)} \right] - 1$$

$$H_2(\lambda) = \lambda \left[\frac{\sinh(2\lambda) - \sin(2\lambda)}{\cosh(2\lambda) - \cos(2\lambda)} \right]$$

$$\delta = 3 \left(\frac{1 - \epsilon}{\epsilon} \right) \frac{L}{U_o} \frac{KD}{R_c^2}$$

$$Pe = \frac{U_o L}{D_L}; \quad y = \frac{2D}{R_c^2}; \quad R_1 = K \left(\frac{1 - \epsilon}{\epsilon} \right)$$

The oscillatory integral in Eq. 12 must be evaluated numerically. A simple rectangular method was used in this study,

with integration continuing until the percentage increase of the integrand was less than a specified tolerance.

Characterization of Silicalite Samples

Silicalite is a synthetic zeolite described first by Flanigen et al. (1978). The solid structure is constructed from tetrahedral SiO_2 building blocks which are arranged to form an anisotropic microporous channel network. Two types of channels are present: straight, elliptical pores (diameter of $5.7 \times 5.1 \text{ \AA}$) along the y direction; sinusoidal, circular pores (diameter of 5.4 \AA) along the x direction. There are no direct channels along the z direction. The channel diameter of silicalite lies between the window size of A and X zeolites.

Two different samples of large laboratory-synthesized silicalite crystals were used in this study. Both were provided by David Hayhurst, who was then at Cleveland State University. Many of the crystals in both samples were twinned, thereby forming small clusters of individual crystals. The first batch of material, designated as sample A, was obtained in limited amount. It was essentially used "as received" since pretreatment losses could not be tolerated. The material was calcined in air at 550°C for four hours. A larger quantity of the second sample (sample B) was available, so pretreatment steps became feasible. The crystals were washed with 0.1 N HCl , filtered, and rinsed, and then the process was repeated with 0.1 N NaOH solution (Hayhurst, 1991). The objective of this procedure was to remove conglomerates of smaller crystals and extraneous material. The crystal clusters were separated into individual crystals by subjecting the sample to a 60-Hz ultrasonic bath for 40 min (Ruthven, 1991). They were then calcined at the same conditions as sample A. The size and shape of the crystals were determined by optical and scanning electron microscopy. A view of a typical crystal of sample A is presented in Figure 1.

The length and width of 325 (sample A) and 230 (sample B) crystals were measured via a computer-interfaced digitizer. Number-based length and width frequency distributions were evaluated from these data and fit with normal distributions determined from least-squares regressions. The effective radius of each crystal, R_c , was evaluated by equating the volume to surface area ratio of a sphere with that of a rectangular parallelepiped in which two dimensions are identical:

$$R_c = \frac{3}{2} \left(\frac{L_c W_c^2}{2L_c W_c + W_c^2} \right) \quad (13)$$

The volume-averaged effective crystal radius distributions presented in Figure 2 were evaluated from these data. Regressed log-normal distributions also plotted in this figure were found to adequately represent the experimental results.

The ultimate objective of the crystal size distribution work was to evaluate the average squared effective crystal radius, $\langle R_c^2 \rangle$, by integrating Eq. 4. This was carried out for the regressed log-normal distributions, resulting in values of $22.5 \mu\text{m}$ (sample A) and $25.37 \mu\text{m}$ (sample B) for $\langle R_c^2 \rangle^{1/2}$. A summary of the size distribution data is presented in Table 1. Although the average effective radii of both samples are relatively similar, the length and width dimensions are substantially different.

The crystals were packed into three different columns with

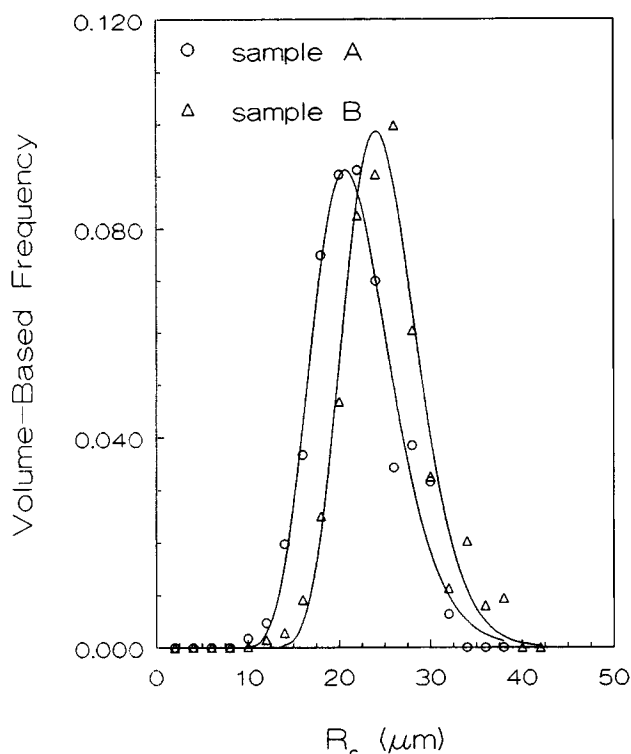


Figure 2. Volume-based effective crystal radius distribution of silicalite samples A and B.

properties as summarized in Table 2. Column names were determined from the silicalite sample letter and the approximate diameter of the column in inches. Uniform packing density was ensured by using vibration during the filling process. The column porosities of systems packed with sample A were found to be much higher than expected—the value for column B-1/8 is much more reasonable. This is likely caused by the clustered nature of silicalite sample A, since the clusters would not pack as efficiently as individual crystals.

Experimental Apparatus

The majority of the data presented in this article were obtained with a Varian GC system described by Hufton and Danner (1993). Both pressure drop and the volumetric flow rate of the carrier gas were measured during each run. Second moments were estimated from values of $w_{1/2}$, which were conveniently determined by the GC system. Regeneration of the solid was carried out overnight by heating the system to 300°C while purging with helium.

Table 1. Crystal-Size Data for Large Laboratory-Synthesized Silicalite Samples

Dimension/Basis/Distribution	Sample A μ_c (μm), σ_c^2	Sample B μ_c (μm), σ_c^2
L_c , number, normal	116, 363	70.6, 184
W_c , number, normal	26.2, 43	36.0, 67
R_c , volume, log-normal	21.6, 0.043	24.8, 0.028
$\langle R_c^2 \rangle^{1/2}$, volume, log-normal	22.5	25.37

Table 2. Characterization of Chromatographic Columns Containing Laboratory-Synthesized Silicalite

Column	D_{col} (mm)	L (cm)	ϵ
A-1/4	4.38	11.15	0.62
A-1/8	2.16	15.56	0.62
B-1/8	2.16	15.79	0.45

A set of runs at low carrier gas velocities was performed in a laboratory-constructed apparatus also described by Hufton and Danner (1991, 1993). This system differed from that above since moments were obtained by integration and vacuum was used for regeneration instead of helium purge. Specific information concerning both chromatographs can be found in the thesis of Hufton (1992).

Experimental Results

Initial investigations measured the transport behavior of methane, ethane, propane, *n*-butane and isobutane in the A-1/4 column at temperatures between 250 and 398 K. Low carrier gas velocities ($U_o < 7$ cm/s) were utilized to minimize the column pressure drop ($\Delta P < 4$ kPa). Second moments were determined by integration (Eq. 1) and then plotted in variance plots. A typical variance plot for propane is shown in Figure 3. Linear regression of these data and comparison with Eq. 5 yielded values of D and D_L . The required values of Henry's constants were obtained from first moments as reported by Hufton and Danner (1993).

The axial dispersion coefficient was found to be independent

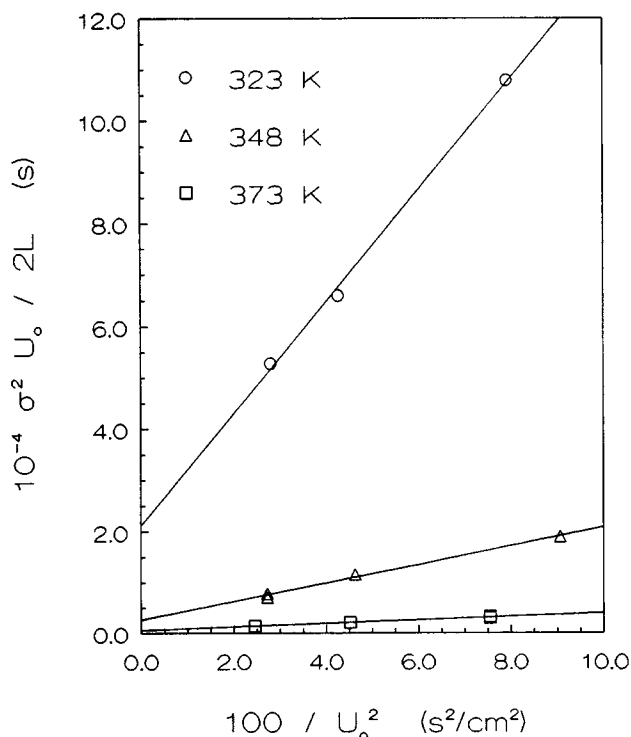


Figure 3. Variance plot for propane on silicalite sample A: isobaric experiments.

of gas velocity, which is the result of the small particle diameter and relatively low gas velocities. Thus, the axial dispersion coefficient could be approximated as:

$$D_L = \tau_L D_m \quad (14)$$

Molecular diffusion coefficients, estimated from Danner and Daubert (1987), were substituted into the above equation to determine values of the dispersion factor, τ_L . The average was found to be 0.84, which is reasonably close to the value of 0.7 mentioned by Ruthven (1984, p. 209).

Micropore diffusion coefficients were estimated from the intercepts of the variance plots. They displayed the expected increase with decreasing chain length and increasing temperature, and were found to be in reasonable agreement with values obtained by ZLC (Eic and Ruthven, 1989), frequency response (Bülow et al., 1986a), and the membrane technique (Hayhurst and Paravar, 1988). Some puzzling inconsistencies were observed, however. The diffusion coefficients of *n*-butane fell below those of isobutane at temperatures greater than 373 K. It was expected that diffusion coefficients of bulkier isobutane would always be lower than those for linear *n*-butane. In addition, values of the activation energy for diffusion, E_a , for the linear alkanes were found to be larger than expected and roughly equal to the heats of adsorption. The value of E_a for isobutane was more reasonable, being significantly smaller than the magnitude of the heat of adsorption. The activation energies were calculated from the slope of plots of $\ln(D)$ vs. $1/T$.

Analysis of the above chromatographic data via the van Deemter approach (Eq. 6) proved that the experiments were conducted at conditions that favored axial dispersion effects. To measure the micropore diffusion resistance more directly, a number of experiments were carried out at higher interstitial gas velocities (up to 60 cm/s). Runs were made with all five alkanes in column A-1/8 and with ethane, propane, and isobutane in column B-1/8. System temperature ranged from 303 to 523 K. These experiments were carried out in the Varian chromatography system, so the $w_{1/2}$ method was used to determine the second moments. The validity of this method was confirmed by comparing some of the results with second moments determined by numerical integration.

Since pressure drops in these runs were appreciable (roughly 50 to 200 kPa), Eq. 8 was used to determine the micropore diffusion coefficients. Experimental HETP data for isobutane in column A-1/8 are plotted in Figure 4. Similar trends were observed with sample B. The slopes of the data at high values of U_o are both significant and temperature-dependent. Micropore diffusion coefficients evaluated from these slopes and Eq. 7 for both silicalite samples are listed in Table 3. The two data sets agree well with each other and are plotted in Figure 5 vs. $1/T$ along with data obtained via the membrane (Paravar and Hayhurst, 1983) and CPC (Chiang et al., 1984b) techniques. The chromatographic data measured in this study compare well with the former, but are more than three orders of magnitude larger than the CPC values. The activation energy determined from the slope of the new chromatographic data were found to be reasonable at 5.80 kcal/mol.

The validity of the parameters determined with the moments technique was checked with time-domain analysis. This procedure was complicated slightly by the nonisobaric nature of

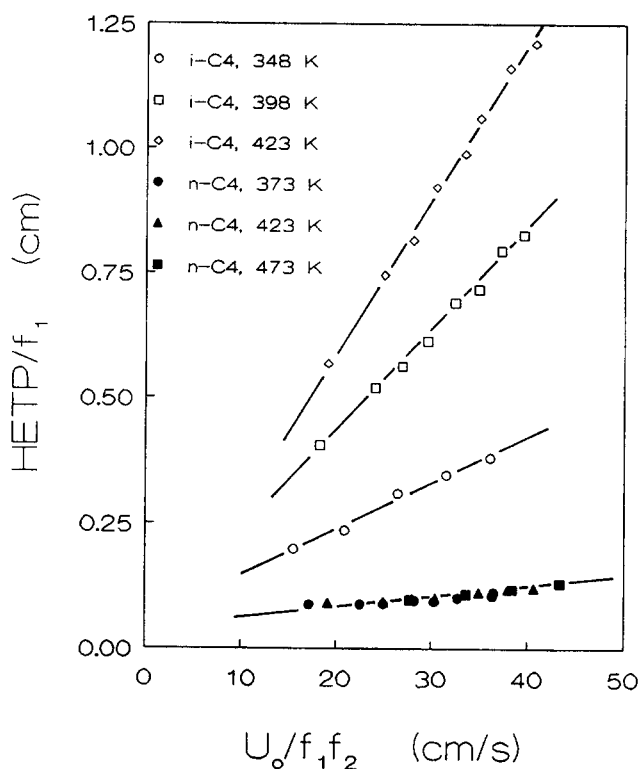


Figure 4. Van Deemter plot for isobutane and *n*-butane in the large laboratory-synthesized silicalite crystals: A-1/8 column, nonisobaric.

the experiments, since the solution given by Eq. 12 assumes constant column pressure. This difficulty was circumvented by replacing the constant gas velocity of Eq. 12 with the average nonisobaric gas velocity, \bar{U} , which is simply U_o/f_2 . A least-squares regression algorithm was used to determine the best value of D from the experimental peaks given the value of D_L (based on $\tau_L = 0.84$). Results for the sample A isobutane runs are listed in Table 3 and plotted in Figure 5. There is very little difference between the moment and the time-domain diffusion coefficients. The fits of the theoretical predictions to the experimental peak data were excellent, as is illustrated in Figure 6 for the 373 K runs.

Plotted in Figure 7 are micropore diffusion coefficients for isobutane calculated with the average crystal width as the characteristic diffusion length instead of the average effective di-

Table 3. Micropore Diffusion Coefficients of Isobutane at Infinite-Dilution on Large Laboratory-Synthesized Silicalite Crystals as Measured via CPC

Sample	<i>T</i> (K)	$10^8 \times D$ (cm ² /s)	
		Moments	Time-Domain
A	348	3.0	2.4
	373	5.6	4.6
	398	9.6	8.0
	423	13.2	12.7
B	373	3.0	—
	398	5.9	—
	423	9.4	—

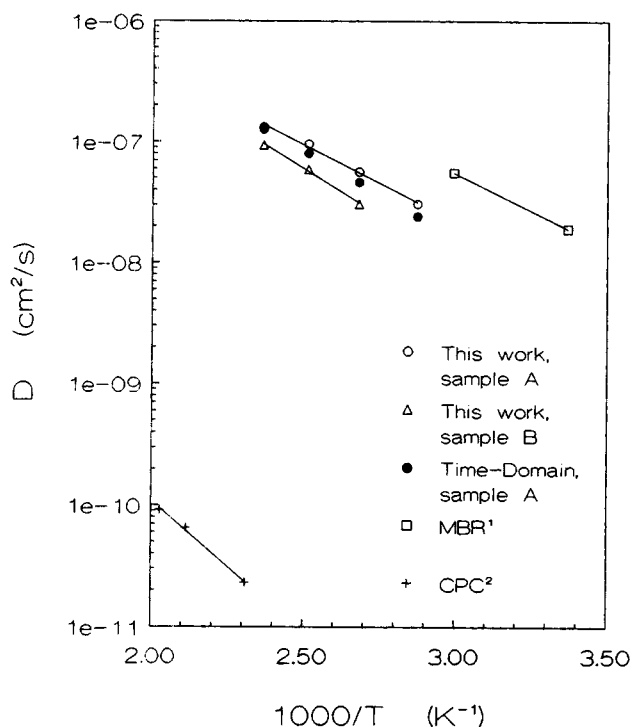


Figure 5. Micropore diffusion coefficients for isobutane in silicalite.

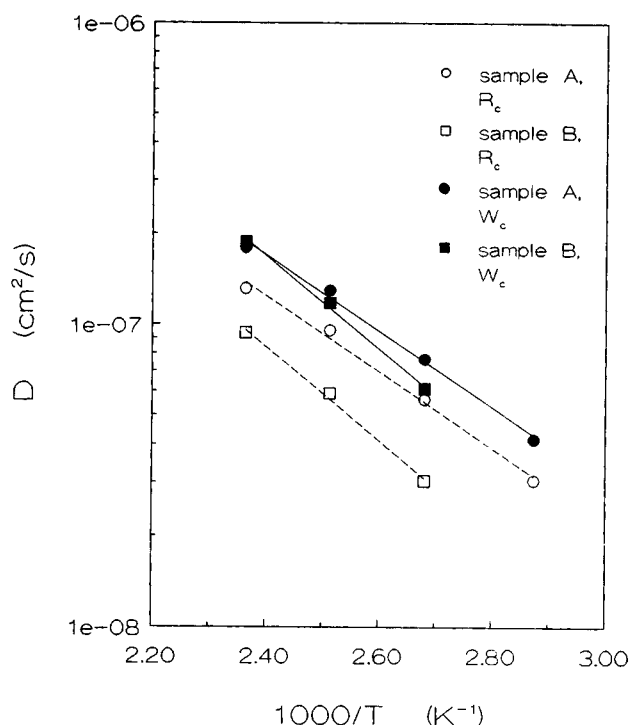


Figure 7. Micropore diffusion coefficients for isobutane in silicalite based on effective crystal diameter and crystal width.

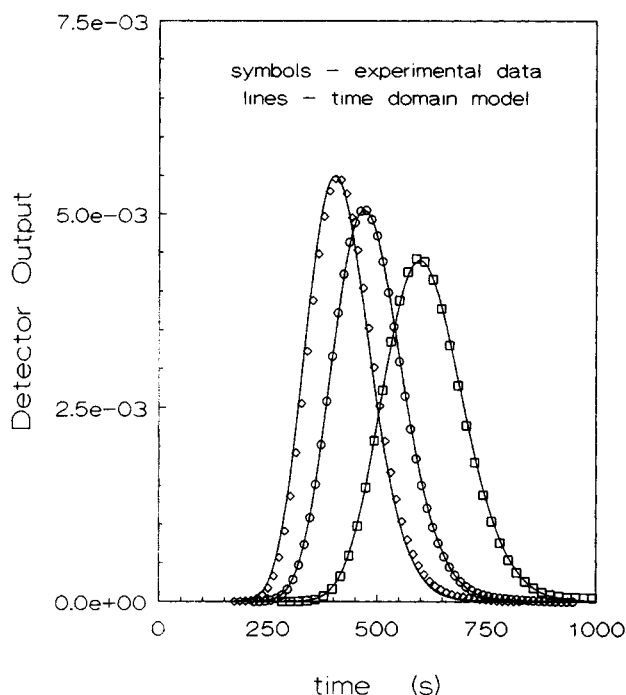


Figure 6. Comparison of experimental isobutane peak data with time-domain regression results: A-1/8 column, nonisobaric, 373 K, $U_0 = 28\text{--}54\text{ cm}^3/\text{min}$.

ameter. This normalization procedure improves the agreement between the sample A and sample B data sets.

Analysis of the linear alkane data via the van Deemter approach showed some startling differences. As illustrated in Figure 4 for *n*-butane on sample A, the HETP data exhibited negligible, temperature-insensitive slopes at high velocities. Similar behavior was observed for other linear alkanes on both samples of adsorbent. The values of D calculated from these van Deemter slopes and Eq. 7 must now be considered effective micropore diffusion coefficients, D_{eff} , since a significant solid-phase resistance was not observed. The values of D_{eff} calculated from these experiments are plotted in Figures 8–11 together with other literature data as given in Table 4. Also illustrated are the results in Table 4. The sources of these data and the identification scheme used in the figures are presented in Table 5. Different degrees of agreement with the literature data can be observed as discussed in the following section.

Interpretation of Experimental Results

The results from this study indicate that the micropore diffusion coefficients of isobutane can be measured accurately via CPC with large laboratory-synthesized crystals. This is possible because the micropore resistance to mass transfer, or $\langle R_c^2 \rangle / KD$, is large. In comparing the expected properties of *n*-butane and isobutane in silicalite, it is not difficult to envision a slower transport rate (smaller value of D) for the bulkier isobutane. Equilibrium effects, however, also contribute to the resistance, since Henry's constants of isobutane were found to be roughly 40% smaller than those for *n*-butane (Hufton and Danner, 1993). Both of these effects act to increase the micropore transport resistance of isobutane.

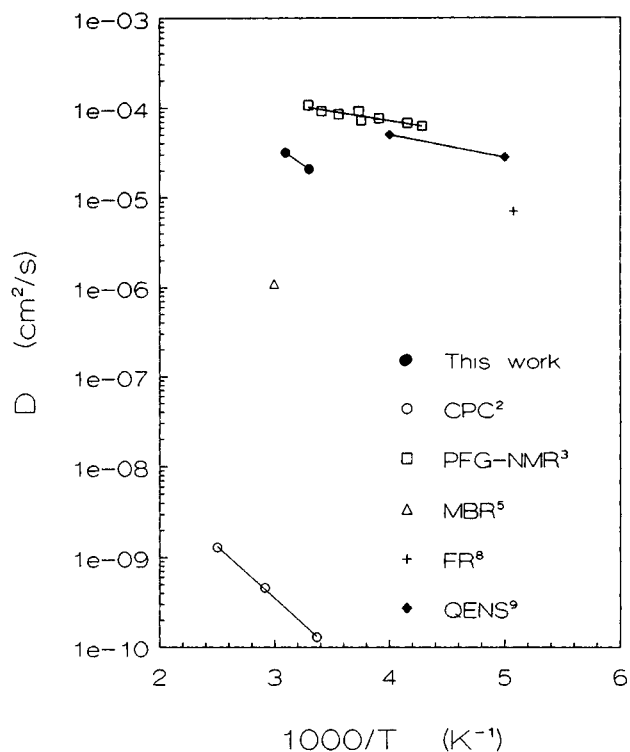


Figure 8. Micropore diffusion coefficients for methane in silicalite.

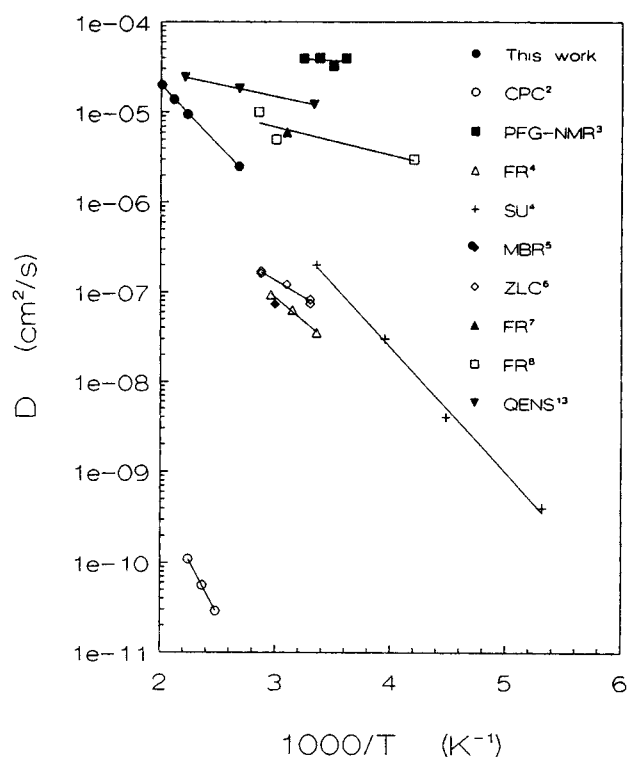


Figure 10. Micropore diffusion coefficients for propane in silicalite.

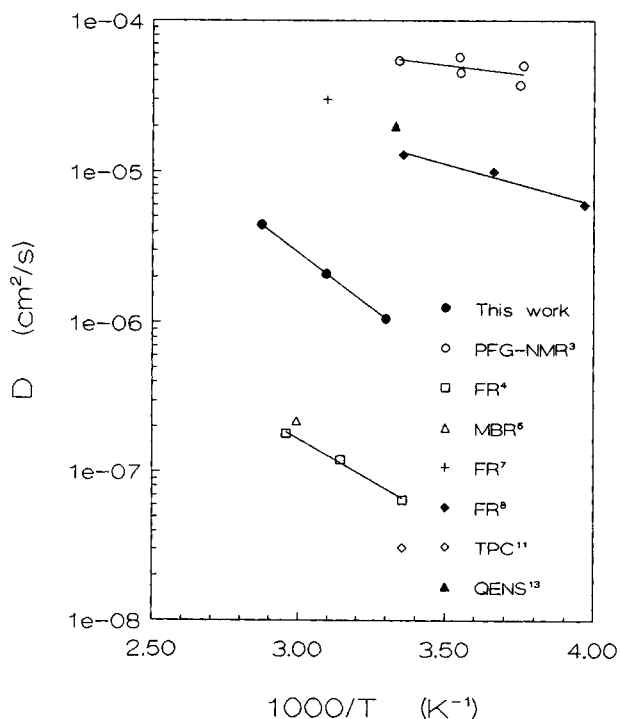


Figure 9. Micropore diffusion coefficients for ethane in silicalite.

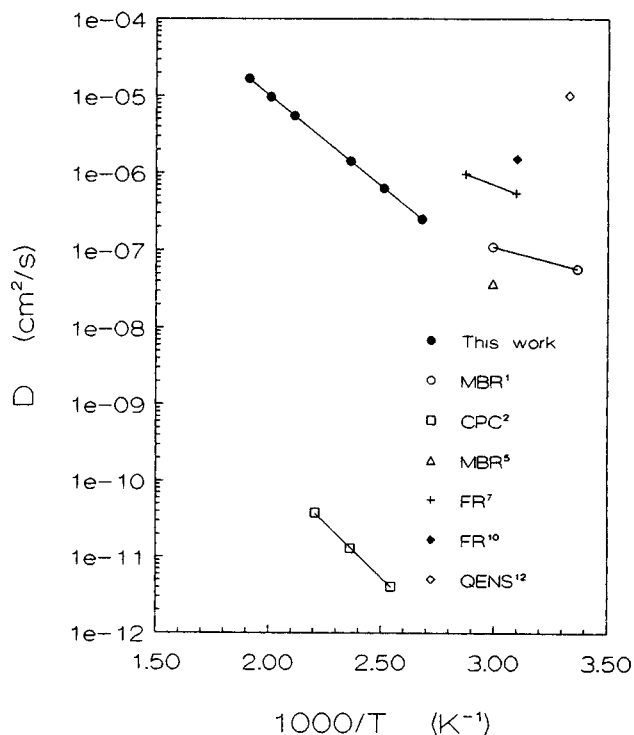


Figure 11. Micropore diffusion coefficients for *n*-butane in silicalite.

Table 4. Summary of C₁-C₄ Alkane Diffusion Data on Silicalite/ZSM-5

<i>T</i> (K)	<i>D</i> (cm ² /s)	Experiment	<i>T</i> (K)	<i>D</i> (cm ² /s)	Experiment
<i>Methane</i>			<i>Propane</i>		
297	1.3×10^{-10}	CPC ²	403	2.9×10^{-11}	CPC ²
343	4.6×10^{-10}	CPC ²	423	5.6×10^{-11}	CPC ²
400	1.3×10^{-9}	CPC ²	446	1.1×10^{-10}	CPC ²
304	1.1×10^{-4}	PFG-NMR ³	308	3.9×10^{-5}	PFG-NMR ³
293	9.2×10^{-5}	PFG-NMR ³	296	4.0×10^{-5}	PFG-NMR ³
281	8.5×10^{-5}	PFG-NMR ³	286	3.2×10^{-5}	PFG-NMR ³
268	9.2×10^{-5}	PFG-NMR ³	277	4.0×10^{-5}	PFG-NMR ³
266	7.2×10^{-5}	PFG-NMR ³	298	3.5×10^{-8}	FR ⁴
256	7.6×10^{-5}	PFG-NMR ³	318	6.3×10^{-8}	FR ⁴
241	6.8×10^{-5}	PFG-NMR ³	338	9.3×10^{-8}	FR ⁴
233	6.2×10^{-5}	PFG-NMR ³	313	1.0×10^{-5}	SU ⁴
334	1.1×10^{-6}	MBR ⁵	298	2.0×10^{-7}	SU ⁴
197	7.0×10^{-6}	FR ⁸	253	3.0×10^{-8}	SU ⁴
200	2.8×10^{-5}	QENS ⁹	223	4.0×10^{-9}	SU ⁴
250	5.0×10^{-5}	QENS ⁹	188	4.0×10^{-10}	SU ⁴
<i>Ethane</i>			334	7.3×10^{-8}	MBR ⁵
299	5.4×10^{-5}	PFG-NMR ³	303	7.4×10^{-8}	ZLC ⁶
282	5.7×10^{-5}	PFG-NMR ³	303	8.2×10^{-8}	ZLC ⁶
282	4.5×10^{-5}	PFG-NMR ³	323	1.2×10^{-7}	ZLC ⁶
266	5.0×10^{-5}	PFG-NMR ³	348	1.6×10^{-7}	ZLC ⁶
267	3.7×10^{-5}	PFG-NMR ³	279	1.7×10^{-7}	ZLC ⁶
298	6.5×10^{-8}	FR ⁴	323	6.0×10^{-6}	FR ⁷
318	1.2×10^{-7}	FR ⁴	351	1.0×10^{-5}	FR ⁸
338	1.8×10^{-7}	FR ⁴	333	5.0×10^{-6}	FR ⁸
334	2.2×10^{-7}	MBR ⁵	238	3.0×10^{-6}	FR ⁸
323	3.0×10^{-5}	FR ⁷	300	1.2×10^{-5}	QENS ¹³
298	1.3×10^{-5}	FR ⁸	373	1.8×10^{-5}	QENS ¹³
273	1.0×10^{-5}	FR ⁸	453	2.4×10^{-5}	QENS ¹³
252	6.0×10^{-6}	FR ⁸	<i>n-Butane</i>		
298	3.1×10^{-8}	TPC ¹¹	297	5.7×10^{-8}	MBR ¹
300	2.0×10^{-5}	QENS ¹³	334	1.1×10^{-7}	MBR ¹
<i>Isobutane</i>			393	4.1×10^{-12}	CPC ²
297	1.9×10^{-8}	MBR ¹	423	1.3×10^{-11}	CPC ²
334	5.5×10^{-8}	MBR ¹	453	3.8×10^{-11}	CPC ²
433	2.3×10^{-11}	CPC ²	334	3.7×10^{-8}	MBR ⁵
473	6.5×10^{-11}	CPC ²	323	5.4×10^{-7}	FR ⁷
493	9.1×10^{-11}	CPC ²	348	9.6×10^{-7}	FR ⁷
			323	1.5×10^{-6}	FR ¹⁰
			300	1.0×10^{-5}	QENS ¹²

Table 5. Key to Sources of Diffusion Data for C₁-C₄ Alkane/Silicalite Systems

Symbol	Reference
MBR ¹	Paravar and Hayhurst, 1983
CPC ²	Chiang et al., 1984b
PFG-NMR ³	Caro et al., 1985
FR ⁴ , SU ⁴	Bülow et al., 1986a
MBR ⁵	Hayhurst and Paravar, 1988
ZLC ⁶	Eic and Ruthven, 1989
FR ⁷	van den Begin and Rees, 1989
FR ⁸	van den Begin et al., 1989
QENS ⁹	Jobic et al., 1989
FR ¹⁰	Shen et al., 1990
TPC ¹¹	Huften and Danner, 1991
QENS ¹²	Jobic et al., 1992a
QENS ¹³	Jobic et al., 1992b

channel network. The two continuous channels in silicalite run along the *x* and *y* directions: to move in the *z* direction an adsorbate must alternatively travel along both channel systems. Computer simulations (June et al., 1990; Huften, 1991) and PFG-NMR measurements (Kärger, 1991) have shown that the amount of transport in the *z* direction is relatively small. As a rough approximation, assume that the resistance to transport along *z* is infinite. A consistent diffusion coefficient will now be obtained only if *D* is based on the characteristic lengths of the *x* and *y* directions. Since these are characterized by the crystal width, the correlation of the diffusion coefficients with crystal width is justified. Infinite resistance to *z* transport, however, is certainly a bold assumption, since transport along both types of channels will necessarily result in some transport along *z* (Kärger, 1991).

The slopes of the linear alkane HETP data at high gas velocity were very small and insensitive to temperature. These observations can be attributed to an insignificant micropore mass-transfer resistance: the values of *D* were too large to be measured via chromatography. The *effective* diffusion coefficients, *D_{eff}*, evaluated from the slopes and Eq. 7 serve as a lower limit of the true micropore diffusion coefficients. Since the slopes were temperature-independent, the temperature dependence of *D_{eff}* is given by $[K(T)]^{-1}$ (Eq. 7), or the measured value of *E_a* is equal to $-\Delta U$ ($\approx -\Delta H$).

The absence of a significant micropore resistance explains the strange observations made with the isobaric data. As above, the measured activation energies for the linear adsorbates were found to be roughly equal to the heats of adsorption. Van Deemter analysis provided insight into the cause of this observation, whereas the variance plots did not reveal any abnormal behavior. Thus, the unambiguous verification of a significant (or insignificant) solid-phase resistance is a major advantage of the van Deemter analysis.

A few generalities can be made concerning the comparison of the linear alkane CPC data of this study with chromatographic results measured by other investigators (Figures 8-11). The infinite-dilution micropore diffusion coefficients of Chiang et al. (1984b) were found to be orders of magnitude smaller than all of the others, and the activation energy was greater than or equal to the heat of adsorption. They used the CPC technique with small commercial silicalite crystals (1 μ m in diameter), so their micropore resistance term was less than 0.1% of this study $[(0.5/20)^2]$. Thus, one would certainly expect their results to exhibit the trends associated with a negligible

The isobutane micropore diffusion coefficients compared well with membrane results, but were much larger than the results of Chiang et al. (1984b). The lack of agreement can be attributed to the small size of the silicalite crystals used by those authors. This behavior was also noted with the linear alkane data.

The successful comparison of parameters determined from moment and time-domain analysis confirms the validity of the moment technique. Since the second moments were estimated from *w_{1/2}* values, this simplified analysis technique is also corroborated. These findings are not entirely surprising, since the chromatographic peaks were found to be nearly symmetrical. The applicability of the isobaric time-domain algorithm to nonisobaric systems was certainly unexpected. Adaptation of the isobaric model to systems with significant pressure drop by using a "corrected" gas velocity appears justifiable for systems similar to those studied.

The fact that the isobutane data were better correlated with the crystal width rather than the effective crystal diameter is apparently caused by the anisotropic nature of the silicalite

micropore resistance. These trends were observed; in fact, even the diffusion coefficients of isobutane could not be measured accurately (Figure 5).

Comparison of the values of D_{eff} for ethane with the results of Hufton and Danner (1991) indicates that the value from the latter is doubtful (TPC^{II}, Figure 9). The silicalite material of Chiang et al. (1984b) was used in this TPC study. Although the experiments were carried out at a high adsorbed-phase concentration, it seems unlikely that this concentration effect would decrease the self-diffusion coefficient to measurable levels. This finding might have been anticipated, since Hufton and Danner showed via time domain analysis that the chromatographic system was not very sensitive to the value of D .

The similarity of the data of Hyun and Danner (1985) with those of Hufton and Danner (1991) suggests that the diffusion coefficients of the former might also be too small. Hyun and Danner measured the values of D_{ethane} at saturation in 13X zeolite via the TPC technique. Like Hufton and Danner (1991), the micropore resistance accounted for only a relatively small percentage of the total. Their value of the ethane self-diffusion coefficient at 298 K in 13X was found to be smaller than that determined in silicalite by Hufton and Danner (7.6×10^{-9} and 3.1×10^{-8} cm²/s, respectively). Since zeolite 13X contains larger pores than does silicalite, the opposite behavior would probably be expected (excluding cation effects). This inconsistency could be the result of experimental analysis of a negligible micropore resistance.

As a lower limit of the true diffusion coefficients, the results measured in this study are inconsistent with extrapolated values obtained from ZLC, membrane, and earlier frequency response experiments (Figures 8–10). The representation of the results of this study as a lower limit, however, is consistent with PFG-NMR and QENS measurements. Thus, the data tend to support the premise that these techniques provide a measure of the true intracrystalline diffusion rate of small alkanes in silicalite.

Further support of the PFG-NMR/QENS data includes relatively recent frequency response results which show a sample-size dependence of the micropore diffusion coefficients. By using silicalite crystals dispersed in glass wool, Van den Begin and Rees (1989) determined diffusion coefficients which were in good agreement with the PFG-NMR/QENS values. Van den Begin et al. (1989) also obtained similar results with the single-step frequency response technique. Beschmann et al. (1990) reported the results of sorption uptake experiments with *n*-nonane and *n*-octane in silicalite at 298 K. Although the precise values of D could not be measured, a lower limit of 1×10^{-6} cm²/s was established. This is higher than the ethane, propane and *n*-butane data determined by MBR, ZLC, TPC and some FR experiments. Finally, recent molecular dynamics simulations of the transport of methane in silicalite have resulted in diffusion coefficients which agree well with PFG-NMR results (June et al., 1990; Hufton, 1991).

Neglecting the early frequency response experiments, the ZLC and membrane diffusion coefficients for the linear alkanes appear to be inconsistent with the CPC lower limit determined in this study. For the membrane experiments an additional process, such as desorption of adsorbate at the low-pressure side of the "membrane," might be responsible for the observed resistance. This may explain why two significantly different results for *n*-butane at 334 K have been determined

by the membrane technique [3.7×10^{-8} cm²/s (Hayhurst and Paravar, 1988) and 1.1×10^{-7} cm²/s (Paravar and Hayhurst, 1983)]. The discrepancy with the ZLC measurements cannot be explained, since the physical process is similar to that employed in the chromatographic experiments.

What can be done in order to accurately measure the diffusion coefficients of the linear alkanes via CPC? The obvious answer is to use larger silicalite crystals to increase the micropore mass-transfer resistance. Crystals roughly an order of magnitude larger than those used in this study would be required to unequivocally determine the diffusion coefficients. Remember also that many of these monodisperse crystals would be required for CPC application. Unfortunately, this type of silicalite sample does not presently exist.

Intuitively, one might suggest decreasing the system temperature to decrease D , thereby slowing the intracrystalline diffusion process. Closer observation of the micropore resistance, though, shows it to be inversely proportional to the product KD , and not just D . If the heat of adsorption is larger than the activation energy for diffusion (which is logical for the alkane/silicalite system), then KD will increase or the micropore resistance will decrease with decreasing temperature. Thus, the magnitude of the micropore resistance can be enhanced by increasing the system temperature.

Another possibility would be to use larger linear alkanes as adsorbate. This would result in lower micropore diffusion coefficients, but higher equilibrium constants at a fixed temperature. Thus, the change in micropore resistance would depend directly on the rate of increase of K and decrease of D with chain length. This approach would probably fail, though, since a lower limit of the diffusion coefficient is expected (Eic and Ruthven, 1989), and the equilibrium constant is an increasing function of chain length (Hufton and Danner, 1993).

Future investigations must involve either experimental techniques which are able to monitor the fast kinetics of the alkane/silicalite system or which make use of specially-prepared samples of very large silicalite crystals. Very large crystals are available, but not in the quantity required for chromatographic investigations (Hayhurst et al., 1989). Thus, experiments which require a modest amount of sample should be used, such as membrane or ZLC techniques. The most important test which must be carried out in these experiments is to vary the size of the silicalite crystal to confirm the significance of micropore resistances. Attainment of a constant micropore diffusion coefficient in these different samples would be compelling evidence that the micropore transport process was being measured.

Conclusions

The bulkiness of isobutane enables one to monitor its progress through silicalite via CPC. A reduction in the diffusion coefficient and Henry's constant resulted in a relatively large micropore resistance which was conclusively determined from van Deemter plots. The diffusion coefficients and activation energies evaluated from this analysis agree with values obtained via the membrane technique. Some evidence of the anisotropic channel structure was observed, since the diffusion coefficients obtained on two different silicalite samples were correlated better with the crystal width instead of the effective diameter.

The transport of linear alkanes through the silicalite channels

occurs at a much faster rate. This was evidenced by van Deemter plots with insignificant slopes at high velocity. These results are still useful, though, since they define a lower limit of the true micropore diffusion coefficients. In this respect, they are inconsistent with values measured via a number of other macroscopic techniques. This lower limit, however, is consistent with the PFG-NMR and QENS values.

Acknowledgment

This work was supported by the National Science Foundation under Grant No. CTS-9101620. We would like to thank David Hayhurst of Cleveland State University for providing the laboratory-synthesized silicalite sample and Douglas Ruthven of the University of New Brunswick for stimulating discussions of this work. The suggestions of Ilyess Hadj Romdhane and experimental assistance of Heather Bergmann are also gratefully acknowledged.

Notation

- a = arbitrary constant
 A, B, H_1, H_2, y, R_1 = constants defined by Eq. 12
 C = gas-phase concentration of adsorbate, mol/cm³
 D = micropore transport diffusion coefficient, cm²/s
 D_{col} = column diameter, cm
 D_L = axial dispersion coefficient, cm²/s
 D_m = molecular diffusion coefficient, cm²/s
 E_a = activation energy for diffusion, cal/mol
 $f(R_c)$ = effective crystal size distribution, dimensionless
 f_1, f_2 = pressure drop correction factors, dimensionless
 $-\Delta H$ = isosteric heat of adsorption, cal/mol
HETP = height equivalent to a theoretical plate, cm
 i = complex number $\sqrt{-1}$
 k_f = external mass-transfer coefficient, cm/s
 K = equilibrium Henry's constant, dimensionless
 L = column length, cm
 L_c = length of crystal, cm
 m = slope of van Deemter plot at high gas velocities, cm/s
 Pe = Peclet number, $U_o L/D_L$, dimensionless
 P_i, P_o = inlet and outlet column pressure, kPa
 R_c = effective crystal radius, cm
 R_p = pellet radius, cm
 $\langle R_c^2 \rangle$ = average squared effective crystal radius, cm²
 s = Laplace variable
 Sh = Sherwood number, $2R_A k_f/D_m$, dimensionless
 t = time, s
 t_b = breakthrough time, s
 T = temperature, K
 t_R = peak retention time, s
 ΔU = change in internal energy upon adsorption, cal/mol
 U_o = interstitial gas velocity evaluated at column outlet conditions, cm/s
 \bar{U} = average interstitial gas velocity for nonisobaric column, cm/s
 $w_{1,2}$ = width of peak at a height equal to half of the maximum peak height, s
 W_c = width of crystal, cm
 x, y, z = Cartesian coordinate axes

Greek letters

- δ = constant defined by Eq. 12
 ϵ = interstitial gas volume/column volume (column porosity), dimensionless
 μ_ξ = mean of size distribution, cm
 σ^2 = peak variance, s²

- σ_c^2 = variance of size distribution, cm²
 τ_L = dispersion factor of Eq. 14, dimensionless

Literature Cited

- Beschmann, K., S. Fuchs, and L. Riekert, "Kinetics of Sorption of Benzene and n-Paraffins in Large Crystals of MFI Zeolites," *Zeolites*, **10**, 798 (1990).
Boniface, H. A., and D. M. Ruthven, "The Use of Higher Moments to Extract Transport Data from Chromatographic Adsorption Experiments," *Chem. Eng. Sci.*, **40**, 1401 (1985).
Bülow, M., H. Schlödder, L. V. C. Rees, and R. E. Richards, "Molecular Mobility of Hydrocarbon ZSM5/Silicalite Systems Studied by Sorption Uptake and Frequency Response Methods," *Proc. Int. Conf. Zeolites*, Tokyo, 579 (1986a).
Bülow, M., H. Schlödder, and P. Struve, "Sorption Uptake of the Molecular Mobility of n-Paraffins in ZSM-5 Type Zeolite," *Adv. Sci. Tech.*, **3**, 229 (1986b).
Bülow, M., W. Miett, P. Struve, and P. Lorenz, "Intracrystalline Diffusion of Benzene in NaX Zeolite Studied by Sorption Kinetics," *J. Chem. Soc., Farad. Trans. 1*, **79**, 2457 (1983).
Carleton, F. B., L. S. Kershenbaum, and W. A. Wakeham, "Adsorption in Non-Isobaric Fixed Beds," *Chem. Eng. Sci.*, **33**, 1239 (1978).
Caro, J., M. Bülow, W. Schirmer, J. Kärger, W. Heink, H. Pfeifer, and S. P. Zdanov, "Microdynamics of Methane, Ethane, and Propane in ZSM-5 Type Zeolites," *J. Chem. Soc., Farad. Trans. 1*, **81**, 2541 (1985).
Chiang, A. S., A. G. Dixon, and Y. H. Ma, "The Determination of Zeolite Crystal Diffusivity by Gas Chromatography: I. Theoretical," *Chem. Eng. Sci.*, **39**, 1451 (1984a).
Chiang, A. S., A. G. Dixon, and Y. H. Ma, "The Determination of Zeolite Crystal Diffusivity by Gas Chromatography: II. Experimental," *Chem. Eng. Sci.*, **39**, 1461 (1984b).
Chihara, K., M. Suzuki, and K. Kawazoe, "Adsorption Rate on Molecular Sieving Carbon by Chromatography," *AIChE J.*, **24**, 237 (1978).
Conder, J. R., and C. L. Young, *Physicochemical Measurement by Gas Chromatography*, Wiley, New York (1979).
Danner, R. P., and T. E. Daubert, *Manual for Predicting Chemical Process Design Data*, AIChE, New York (1987).
Doelle, H.-J., J. Heering, L. Riekert, and L. Marosi, "Sorption and Catalytic Reaction in Pentasil Zeolites. Influence of Preparation and Crystal Size on Equilibria and Kinetics," *J. Cat.*, **71**, 27 (1981).
Edwards, M. F., and J. F. Richardson, "Gas Dispersion in Packed Beds," *Chem. Eng. Sci.*, **23**, 109 (1968).
Eic, M., and D. M. Ruthven, "Diffusion of Linear Paraffins and Cyclohexane in NaX and 5A Zeolite Crystals," *Zeolites*, **8**, 472 (1988).
Eic, M., and D. M. Ruthven, "Intracrystalline Diffusion of Linear Paraffins and Benzene in Silicalite Studied by the ZLC Method," *Zeolites: Facts, Figures, Future*, P. A. Jacobs and R. A. van Santen, eds., Elsevier Science Publishers, Amsterdam (1989).
Eic, M., M. Goddard, and D. M. Ruthven, "Diffusion of Benzene in NaX and Natural Faujasite," *Zeolites*, **8**, 327 (1988).
Fahim, M. A., and N. Wakao, "Parameter Estimation from Tracer Response Measurements," *Chem. Eng. J.*, **25**, 1 (1982).
Flanigen, E. M., J. M. Bennett, R. W. Grose, J. P. Cohen, R. L. Patton, A. M. Kirchner, and J. V. Smith, "Silicalite, a New Hydrophobic Crystalline Silica Molecular Sieve," *Nat.*, **271**, 512 (1978).
Fu, C., M. S. P. Ramesh, and H. W. Haynes, Jr., "Analysis of Gas Chromatography Pulse Dispersion Data for the System n-Butane/Zeolite NaY," *AIChE J.*, **32**, 1848 (1986).
Giddings, J. C., *Dynamics of Chromatography Part I: Principles and Theory*, Marcel Dekker, New York (1965).
Hashimoto, N., and J. M. Smith, "Macropore Diffusion in Molecular Sieve Pellets by Chromatography," *Ind. Eng. Chem. Fundam.*, **12**, 353 (1973).
Hayhurst, D. T., personal communication (1991).
Hayhurst, D. T., P. J. Melling, W. J. Kim, and W. Bibbey, "Effect of Gravity on Silicalite Crystallization," *ACS Symp. Ser.*, No. 398, 233 (1989).
Hayhurst, D. T., and A. D. Paravar, "Diffusion of C₁ to C₅ Normal Paraffins in Silicalite," *Zeolites*, **8**, 27 (1988).

- Haynes, H. W., Jr., "The Determination of Effective Diffusivity by Gas Chromatography: Time Domain Solutions," *Chem. Eng. Sci.*, **30**, 955 (1975).
- Haynes, H. W., Jr., and P. N. Sarma, "A Model for the Application of Gas Chromatography to Measurements of Diffusion in Bidisperse Structured Catalysts," *AIChE J.*, **19**, 1043 (1973).
- Helfferich, F., and G. Klein, *Multicomponent Chromatography*, Marcel Dekker, New York (1970).
- Hsu, L.-K. P., and H. W. Haynes, Jr., "Effective Diffusivity by the Gas Chromatography Technique: Analysis and Application to Measurements of Diffusion of Various Hydrocarbons in Zeolite NaY," *AIChE J.*, **27**, 81 (1981).
- Huften, J. R., "Analysis of the Adsorption of Methane in Silicalite by a Simplified Molecular Dynamics Simulation," *J. Phys. Chem.*, **95**, 8836 (1991).
- Huften, J. R., "Diffusion and Equilibrium Parameters of Alkanes on Silicalite Determined by Perturbation Chromatography," PhD Diss., Pennsylvania State Univ. (1992).
- Huften, J. R., and R. P. Danner, "Gas-Solid Diffusion and Equilibrium Parameters by Tracer Pulse Chromatography," *Chem. Eng. Sci.*, **46**, 2079 (1991).
- Huften, J. R., and R. P. Danner, "Chromatographic Study of Alkanes in Silicalite: Equilibrium Properties," *AIChE J.*, **39**, 954 (1993).
- Hyun, S. H., and R. P. Danner, "Adsorption Equilibrium Constants and Intraparticle Diffusivities in Molecular Sieves by Tracer-Pulse Chromatography," *AIChE J.*, **31**, 1077 (1985).
- James, A. T., and A. J. P. Martin, "Gas-Liquid Partition Chromatography: the Separation and Micro-estimation of Volatile Fatty Acids from Formic Acid to Dodecanoic Acid," *Biochem. J.*, **50**, 679 (1952).
- Jobic, H., M. Bee, and G. J. Kearley, "Translational and Rotational Dynamics of Methane in ZSM-5 Zeolite: A Quasi-Elastic Neutron Scattering Study," *Zeolites*, **9**, 312 (1989).
- Jobic, H., M. Bee, and J. Caro, "Translational Mobility of n-Butane and n-Hexane in ZSM-5 Measured by Quasi-Elastic Neutron Scattering," *Int. Zeolite Conf.*, Montreal (July 5-10, 1992a).
- Jobic, H., M. Bee, and G. J. Kearley, "Dynamics of Ethane and Propane in Zeolite ZSM-5 Studied by Quasi-Elastic Neutron Scattering," *Zeolites*, **12**, 146 (1992b).
- June, R. L., A. T. Bell, and D. N. Theodorou, "Molecular Dynamics Study of Methane and Xenon in Silicalite," *J. Phys. Chem.*, **94**, 8232 (1990).
- Kärger, J., "Random Walk through Two-Channel Networks: A Simple Means to Correlate the Coefficients of Anisotropic Diffusion in ZSM-5 Type Zeolites," *J. Phys. Chem.*, **95**, 5558 (1991).
- Kärger, J., and J. Caro, "Interpretation and Correlation of Zeolite Diffusivities Obtained from Nuclear Magnetic Resonance and Sorption Experiments," *J. Chem. Soc., Farad. Trans. 1*, **73**, 1363 (1977).
- Kärger, J., and H. Pfeifer, "N.M.R. Self-Diffusion Studies in Zeolite Science and Technology," *Zeolites*, **7**, 90 (1987).
- Kärger, J., and H. Pfeifer, "Transport Properties of Molecular Sieves Studied by the NMR Pulsed Field Gradient Technique," *Perspectives in Molecular Sieve Science*, Amer. Chem. Soc., 376 (1988).
- Kärger, J., H. Pfeifer, D. Freude, J. Caro, M. Bülow, and G. Ohlmann, "NMR Investigations of Self-Diffusion in Pentasils," *Proc. Int. Conf. Zeolites*, 633 (1986).
- Kärger, J., H. Pfeifer, and W. Heink, "NMR Diffusion Studies in Zeolites," *Proc. Int. Conf. Zeolites*, 184 (1983).
- Kärger, J., and D. M. Ruthven, "Diffusion in Zeolites," *J. Chem. Soc., Farad. Trans. 1*, **77**, 1485 (1981).
- Kärger, J., and D. M. Ruthven, "On the Comparison Between Macroscopic and NMR Measurements of Intracrystalline Diffusion in Zeolites," *Zeolites*, **9**, 267 (1989).
- Knöblach, K., "Pressure-Swing Adsorption: Geared for Small-Volume Users," *Chem. Eng.*, **85**(25), 87 (1978).
- Ma, Y. H., and C. Mancel, "Diffusion Studies of CO₂, NO, NO₂, and SO₂ on Molecular Sieve Zeolites by Gas Chromatography," *AIChE J.*, **18**, 1149 (1972).
- Ma, Y. H., and C. Mancel, "Diffusion of Hydrocarbons in Mordenites by Gas Chromatography," *ACS Adv. Chem. Ser.*, No. 121, 392 (1973).
- Ma, Y. H., and L. A. Savage, "Xylene Isomerization Using Zeolites in a Gradientless Reactor System," *AIChE J.*, **33**, 1233 (1987).
- Paravar, A., and D. T. Hayhurst, "Direct Measurement of Diffusivity for Butane Across a Single Large Silicalite Crystal," *Proc. Int. Conf. Zeolites*, 217 (1983).
- Qureshi, W. R., and J. Wei, "One- and Two-Component Diffusion in Zeolite ZSM-5: II. Experimental," *J. Cat.*, **126**, 147 (1990).
- Radeke, K.-H., "Critical Remarks on Using Moments Method," *Ind. Eng. Chem. Fundam.*, **20**, 302 (1981).
- Rasmuson, A., "Exact Solution of a Model for Diffusion and Transient Adsorption in Particles and Longitudinal Dispersion in Packed Beds," *AIChE J.*, **27**, 1032 (1981).
- Rasmuson, A., "Time Domain Solution of a Model for Transport Processes in Bidisperse Structured Catalysts," *Chem. Eng. Sci.*, **37**, 787 (1982).
- Rasmuson, A., "Exact Solution of a Model for Diffusion in Particles and Longitudinal Dispersion in Packed Beds: Numerical Evaluation," *AIChE J.*, **31**, 518 (1985).
- Rasmuson, A., and I. Neretnieks, "Exact Solution of a Model for Diffusion in Particles and Longitudinal Dispersion in Packed Beds," *AIChE J.*, **26**, 686 (1980).
- Ruthven, D. M., "Diffusion in Molecular Sieves: A Review of Recent Developments," *ACS Symp. Ser.*, No. 40, 320 (1977).
- Ruthven, D. M., *Principles of Adsorption and Adsorption Processes*, Wiley, New York (1984).
- Ruthven, D. M., personal communication (1991).
- Ruthven, D. M., and R. Kumar, "A Chromatographic Study of the Diffusion of N₂, CH₄, and Binary CH₄-N₂ Mixtures in 4A Molecular Sieve," *Can. J. Chem. Eng.*, **57**, 342 (1979).
- Schneider, P., "Accuracy of Chromatographic Moments—Effects of Peak Treatment and Approximations," *Chem. Eng. Sci.*, **42**, 1251 (1987).
- Schneider, P., and J. M. Smith, "Adsorption Rate Constants from Chromatography," *AIChE J.*, **14**, 762 (1968).
- Shah, D. B., D. T. Hayhurst, G. Evanina, and C. J. Guo, "Sorption and Diffusion of Benzene in HZSM-5 and Silicalite Crystals," *AIChE J.*, **34**, 1713 (1988).
- Shah, D. B., and D. M. Ruthven, "Measurement of Zeolitic Diffusivities and Equilibrium Isotherms by Chromatography," *AIChE J.*, **23**, 804 (1977).
- Shen, D., L. V. C. Rees, J. Caro, M. Bülow, B. Zibrowius, and H. Jobic, "Diffusion of C₄ Hydrocarbons in Silicalite-1," *J. Chem. Soc. Farad. Trans.*, **86**, 3943 (1990).
- Suzuki, M., and J. M. Smith, "Axial Dispersion in Beds of Small Particles," *Chem. Eng. J.*, **3**, 256 (1972).
- van Deemter, J. J., F. J. Zuiderweg, and A. Klinkenberg, "Longitudinal Diffusion and Resistance to Mass Transfer as Causes of Nonideality in Chromatography," *Chem. Eng. Sci.*, **5**, 271 (1956).
- van den Begin, N. G., and L. V. C. Rees, "Diffusion of Hydrocarbons in Silicalite Using a Frequency-Response Method," *Zeolites: Facts, Figures, Future*, P. A. Jacobs and R. A. van Santen, eds., Elsevier, Amsterdam, 915 (1989).
- van den Begin, N., L. V. C. Rees, J. Caro, and M. Bülow, "Fast Adsorption-Desorption Kinetics of Hydrocarbons in Silicalite-1 by the Single-Step Frequency Response Method," *Zeolites*, **9**, 287 (1989).
- Wakao, N., and T. Funazkri, "Effect of Fluid Dispersion Coefficients on Particle to Fluid Mass Transfer Coefficients in Packed Beds," *Chem. Eng. Sci.*, **33**, 1375 (1978).
- Wakao, N., S. Kaguei, and J. M. Smith, "Adsorption Chromatography Measurements. Parameter Determination," *Ind. Eng. Chem. Fundam.*, **19**, 363 (1980).
- Wernick, D. L., and E. J. Osterhuber, "Diffusional Transition in Zeolite NaX: 1. Single Crystal Gas Permeation Studies," *Proc. Int. Conf. Zeolites*, 122 (1983).
- Wu, P., A. Debebe, and Y. H. Ma, "Adsorption and Diffusion of C₆ and C₈ Hydrocarbons in Silicalite," *Zeolites*, **3**, 118 (1983).
- Yang, R. T., *Gas Separation by Adsorption Processes*, Butterworths, Boston (1987).
- Yasuda, Y., "Determination of Vapor Diffusion Coefficients in Zeolite by the Frequency Response Method," *J. Phys. Chem.*, **86**, 1913 (1982).
- Yasuda, Y., and G. Sugawara, "A Frequency Response Technique to Study Zeolitic Diffusion of Gases," *J. Cat.*, **88**, 530 (1984).
- Zikanova, A., M. Bülow, and H. Schlödder, "Intracrystalline Diffusion of Benzene in ZSM-5 and Silicalite," *Zeolites*, **7**, 115 (1987).

Manuscript received May 18, 1992, and revision received Dec. 18, 1992.